Binding of Organometallic Ruthenium(II) Anticancer Compounds to Nucleobases: A Computational Study†

Christian Gossens, Ivano Tavernelli, and Ursula Rothlisberger*

Institut des Sciences et Ingénierie Chimiques, Ecole Polytechnique Fédérale de Lausanne (EPFL), CH-1015 Lausanne, Switzerland

Received: April 8, 2009; Revised Manuscript Received: September 11, 2009

The reaction of the anticancer compound $[(\eta^6\text{-benzene})Ru(en)(OH_2)]^{2+}$ (**1**) toward the nucleobases guanine, adenine, and cytosine is studied computationally using DFT/BP86 calculations. The aqua leaving group of such compounds is known to undergo ligand exchange reactions with nucleophilic centers in DNA and preferentially with the N7 atom of guanine, N7(G). Our results show that an H-bonded reactant adduct with nucleobases is formed via either the aqua ligand (cis adduct) or the en (ethylenediamine) ligand (trans adduct) of **1**. All studied nucleobases favor an H-bonded cis adduct. Only guanine forms also a trans reactant adduct in the gas phase. The guanine N7 and O6 atoms in this trans adduct are situated in an ideal position to form each a strong H-bond to both amino groups of the en ligand of **1**. A docking study shows that this unique recognition pattern is also plausible for the interaction with double stranded DNA. For the reaction of **1** with guanine, we identified three different reaction pathways: (i) A cis (G)N7−Ru−OH_2 transition state (TS). (ii) A direct trans reaction pathway. (iii) A 2-step trans mechanism. The activation energies for the cis pathway are smaller than for the trans pathways. The ultimately formed Ru−N7(G) product is characterized by a thermally stable H-bond between the O6(G) and a diamine-NH_2 hydrogen.

Introduction

Since its discovery in 1965, cisplatin $[Pt(NH_3)_2(Cl)_2]$ has become one of the most important clinical anticancer drugs.[1−3] The remaining limitations of its therapeutic application, namely high toxicity, lack of selectivity, and occurrence of resistance,[4] have stimulated inorganic chemists to search for other transition metal complexes with improved therapeutic profiles.[5−8] However, so far only very similar compounds such as carboplatin and oxaliplatin have made their way into general clinical use.[9] Recently, ruthenium complexes have attracted particular attention as potential alternatives for cisplatin.[10] The ruthenium based compound NAMI-A[11] for instance, prevents the development and growth of pulmonary metastases in solid tumors without activity against primary tumors.[12] Both NAMI-A and a second compound named KP1019, which induces apoptosis in colorectal carcinoma, have completed phase I clinical trials.[13,14] However, multiple ligand exchange reactions of inorganic ruthenium compounds in the physiological environment are often complicating their application as well-defined drugs.[15]

Therefore, more inert organoruthenium compounds have moved into the focus of anticancer research recently.[16] These complexes are based on a ruthenium(II) containing organometallic moiety of the type $[(\eta^6\text{-arene})Ru]^{2+}$,[17−22] $[(\eta^5\text{-cyclopentadienyl})Ru]^{+}$,[23,24] or $[(1,4,7\text{-trithiacyclononane})Ru]^{2+}$.[25] Various monodentate or chelating ligands can occupy the remaining three coordination sites in these pseudo-octahedral complexes, which exhibit a so-called "piano stool" geometry. Currently, intensive experimental research is concentrated on $[(\eta^6\text{-arene})Ru(en)(Cl)]^{+}$ (where en = ethylenediamine).[26,27] Like cisplatin, the chloro complex of this compound hydrolyzes only at very low chloride concentrations (e.g., inside a human cell), while no hydrolysis occurs at higher chloride concentrations (e.g., in the human bloodstream),[28] and DNA is considered to be the most relevant biological target.[29,30] This is further supported by experiments that have shown that a hydrolyzed ruthenium-arene-diamine can indeed bind to an oligonucleotide. Crystal structures have been determined that show a ruthenium−N7 bond between guanine derivatives and $[(\eta^6\text{-arene})Ru(en)]^{2+}$ (arene = biphenyl; 5,8,9,10-tetrahydroanthracene or 9,10-dihydroanthracene). In crystallographic and NMR studies, arene−nucleobase stacking and a stereospecific hydrogen bond of an en−NH_2 hydrogen to the guanine C6═O has been observed. These interactions have been suggested to be at the origin of the higher selectivity toward the N7 atom of guanine than the one observed for cisplatin.[31,32] In contrast, interactions of the en-NH_2 group with the C6−NH_2 group of adenine were shown to be repulsive.[33]

Besides this, little atomistic knowledge is available about the steps involved from hydrolysis to DNA binding of $[(\eta^6\text{-arene})Ru(en)(Cl)]^{+}$. In a recent study on related organoruthenium compounds, we have shown that computational approaches can help rationalizing experimental results and even guide experimental work on these systems.[34,35] The reaction pathway from the Ru−aqua complex to the Ru−DNA adduct is of potential importance for future drug design and lead optimization. Once the crucial drug−DNA interactions are identified, rational structural optimization of **1** will hopefully yield compounds with improved activity profiles. Experiments have demonstrated that in the presence of DNA nucleobases (guanine (G), adenine (A), cytosine (C), and thymine (T)), the selectivity of $[(\eta^6\text{-benzene})Ru(en)(OH_2)]^{2+}$ (**1**, Ru−aqua) to guanine is nearly exclusive, clearly exceeding that of cisplatin.

In the first part of the present study, we reduced the complex reaction of **1** with nuclear DNA to the reaction with guanine in gas phase and in a continuum solvent. Subsequently, we docked the found adducts and transition states to B-DNA. Finally, we investigated the interactions of **1** with adenine and cytosine. In

† Part of the "Walter Thiel Festschrift".

* E-mail ursula.roethlisberger@epfl.ch.

10.1021/jp903237w CCC: $40.75
Published on Web 09/30/2009

the absence of explicit solvent, we decided not to investigate the deprotonated N3−thymine species ($pK_a > 9.5$) in the gas phase as this would involve an unsolvated, negatively charged ligand.

Computational Details

Except as stated otherwise, all calculations were carried out using density functional theory (DFT) at the generalized gradient approximation (GGA) level of theory as implemented in the ADF 2004.01 package.[36] The BP86[37,38] exchange−correlation energy functional and the "TZP" basis set of the ADF package were used. This basis set is of triple-ζ quality with one polarization function in the valence region and a double-ζ representation for the core. The frozen core approximation (for electrons up to main quantum number $n = 1$ for C, N, O and up to $n = 3$ for Ru) and a spin-restricted formalism were applied. As shown in previous calculations, the investigated compounds can be treated as closed shell systems.[34] The ZORA approach was used to incorporate scalar relativistic effects.[39] The general numerical integration (gni) precision parameter was generally increased to 5.0 and we applied tighter convergence criteria (energy, $E = 10^{-4}$ hartree; gradients, Grad $= 3 \times 10^{-3}$ hartree/Å; Cartesian coordinates, Coord $= 3 \times 10^{-3}$ Å) as the default values are not sufficient for a proper convergence. This is true in particular for the transition state search algorithm (eigenvector following approach) for which even tighter criteria (gni ≥ 7.0, $E = 10^{-5}$ hartree; Grad $= 10^{-3}$ hartree/Å; Coord $= 10^{-3}$ Å) were applied. Forces in the frequency analysis were calculated via a 2-point numerical differentiation with gni = 6.0. All transition states were characterized by a single imaginary mode. COSMO calculations were conducted on gas phase geometries (gni = 7.0, parameters as in ref 18) to estimate aqueous solvation effects.

In addition, we performed Car−Parrinello molecular dynamics (CPMD) calculations with the CPMD program.[40] In this case, an analytical local pseudopotential (PP) for hydrogen atoms and nonlocal, norm-conserving soft PPs of the Martins−Trouiller[41] type for all other elements were used.[42] The explicitly treated valence electrons were kept equal to the ones used in the ADF calculations. The PP for ruthenium incorporates scalar relativistic effects.[43] The PPs for C, N, and O were transformed to a fully nonlocal form using the scheme of Kleinman and Bylander,[44] whereas for Ru the semicore PP was integrated numerically using a Gauss−Hermite quadrature. The BP86 exchange−correlation energy functional was used with an energy cutoff of 75 Ry, a time step of 4 au (0.097 fs), a fictitious electron mass of 400 au, an orbital convergence of 10^{-6} au and a temperature of 310 K (except where stated differently). Simulations were started from ADF geometry preoptimized structures.

For the qualitative dsDNA docking studies we employed the sequence d(CCTCTG*GTCTCC)/ d(GGAGACCAGAGG) where G* is the reaction site to which we fitted the guanine ligand of the ruthenium complexes.[45,46] An equilibrated configuration was taken from a mixed classical/quantum molecular dynamics (MD) simulation of a fully solvated and charge-neutralized DNA adduct of the $[(\eta^6\text{-arene})Ru(en)]^{2+}$ moiety in the major groove of dsDNA.[45−47] Figures were done with Molekel[48] and VMD.[49]

Resuts and Discussion

1. Reaction of the Ru−Aqua Compound with Guanine. ***1.1. H-bonded Adducts of Guanine with $[(\eta^6$-benzene)Ru(en)$(OH_2)]^{2+}$.*** Both the guanine base and the Ru−aqua complex contain numerous H-bond donor and acceptor sites. There are four H-bond donors in the en ligand, two donors in the aqua ligand and four donors as well as three acceptors in guanine (Scheme 1). Therefore, it is chemically plausible that the ligand exchange reaction of Ru−L (L = OH_2 vs N7(G)) initially proceeds via the formation of an H-bonded reactant adduct. To sample all degrees of freedom on this highly nontrivial potential energy surface (PES) in an unbiased way, we performed unconstrained in vacuo Car−Parrinello molecular dynamics (CPMD) simulations to identify the most stable H-bonded adducts. First we placed the guanine on the aqua side of the ruthenium complex (cis) with the guanine O6 and N7 atoms H-bonding to the aqua hydrogens Hw1 and Hw2 (Figure 1). A second simulation was started with the guanine placed on the diamine side of the ruthenium complex, opposite to the aqua ligand (trans). This configuration allows both guanine O6 and N7 atoms to form each a hydrogen bond to one of the en-NH_2 groups (Figure 2).

SCHEME 1: Aqua vs Nucleobase Ligand Exchange Reaction of $[(\eta^6$-benzene)Ru(en)$(OH_2)]^{2+}$ (1)

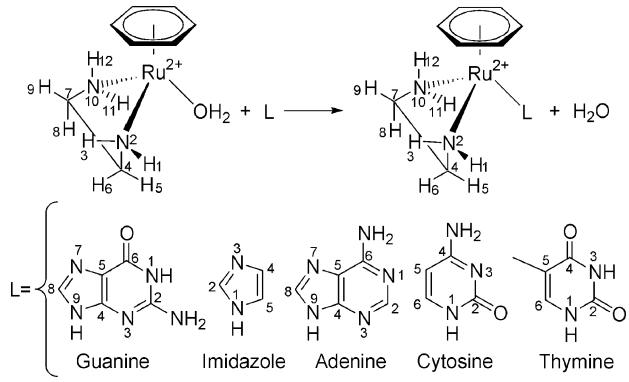

1.1.1. Cis Ru−Aqua/Guanine Adduct. Placing the incoming guanine on the same side as the aqua ligand of the ruthenium complex, we observed an attraction between both molecules. The two hydrogens of the aqua ligand form two very stable H-bonds, namely to the N7 and the C═O6 atoms of guanine (Figure 1). These H-bonds and the ruthenium-aqua coordination bond are stable on the time scale of our CPMD dynamics at 310 K (Figure S1, Supporting Information). The bond between ruthenium and the aqua oxygen (O_{aq}) is not perturbed by the presence of the new H-bonds. In contrast, the O_{aq}−H bond lengths of the aqua ligand are elongated whenever the guanine H-bond acceptor atoms, N7 and O6, come very close to the aqua hydrogens. However, at no time do the latter two show any tendency for a proton transfer reaction. The O6(G) is involved in H-bonding to the en-N1, whereas the N7(G) does not interact with the corresponding en-H12 atom. Both the Ru−N7 and Ru−O6 distances stabilize around 4.5 Å (Figure S2, Supporting Information). During our short dynamics we did not observe any tendency for a spontaneous ligand exchange reaction.

Further annealing followed by geometry optimization yielded the structure in Figure 1, which corresponds to the lowest minimum on the PES for an H-bonded adduct. As a consequence of the H-bonds between guanine and the aqua ligand, both aqua hydrogen−oxygen bonds are slightly elongated compared to the isolated aqua complex (1.03 vs 0.98 Å) and the Ru−O_{aqua} bond is significantly shortened (2.13 Å vs 2.26 Å). The O6(G) forms an H-bond not only to the Hw1 but also to the en-H1. This explains the higher stability of the O6−Hw1 H-bond during the CPMD simulation compared to the N7−Hw2 H-bond.

1.1.2. Trans Ru−Aqua/Guanine Adduct. A second stable local minimum was identified in our CPMD simulations, in

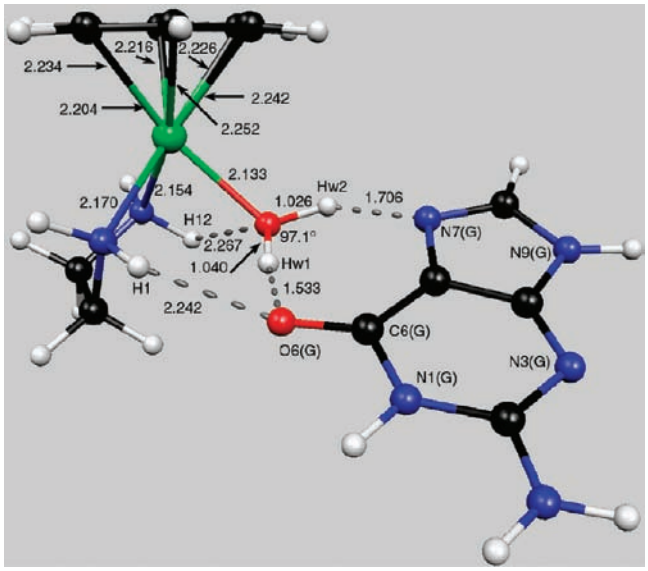

Figure 1. Geometry optimized H-bonded cis reactant adduct of guanine with **1**.

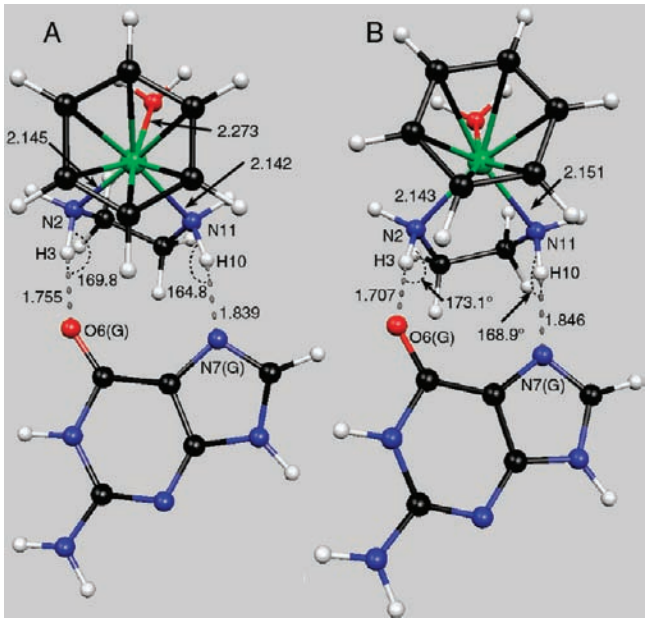

Figure 2. Geometry optimized H-bonded trans adducts of guanine to diamine in **1**. Depicted are the less stable diamine conformer (A) and the slightly more stable (0.3 kcal/mol) conformer (B) resulting from a dihedral angle flip of the en ligand.

which the guanine ligand approaches the [(η^6-benzene)Ru(en)(OH_2)]$^{2+}$ complex from the diamine side, i.e., trans to the aqua ligand. In this adduct, the guanine can form strong H-bonds to the diamine ligand via its N7 and O6 atoms (Figure 2). These hydrogen bonds were stable on the time scale of our CPMD simulations (Figure S3, Supporting Information). The distances between the ruthenium center and the guanine N7 and O6 atoms are similar for the cis and trans adducts. It is worth mentioning that the O6(G) is for both the cis and the trans adduct on average closer to the ruthenium center than the N7(G) atom, which ultimately coordinates to ruthenium in the final reaction product. As can be seen from Figure 3, we observed a barrier-free rotation of the arene ligand during our simulation. In fact, the arene ligand completes a full 360° rotation within 2 ps simulation. This is the consequence of the corresponding potential energy profile that we reported elsewhere.[33] Therefore, ruthenium

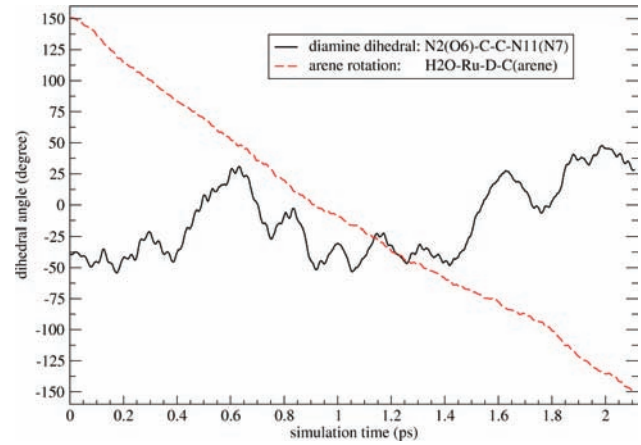

Figure 3. NCCN ethylenediamine dihedral angle (deg) and arene rotation (D = centroid of benzene ring) during a CPMD simulation of the reactant adduct in which guanine is oriented trans to **1**.

complexes containing modified arenes can adapt to, e.g., a DNA environment by simple arene rotation. Another interesting aspect is related to the observation of a flip of the diamine NCCN dihedral angle from around −40° to +40°. As was suggested on the basis of the corresponding potential energy profile,[47] the diamine ligand can sample both possible conformers, which differ only slightly in energy. Even on the short time scale of our simulation, the dihedral flips spontaneously to the more stable diamine conformer (Figure 2).[47] Again, this intrinsic conformational flexibility should facilitate the reaction of **1** with dsDNA.

Subsequent geometry optimizations of CPMD snapshots yielded the structures reported in Figure 2. Structure A corresponds to the initial dihedral angle in our simulation and its potential energy is ∼0.3 kcal/mol higher than that of structure B. Overall, the trans reactant adduct is less stable than the cis adduct both in the gas phase (16.1 kcal/mol) and in aqueous solution (13.2 kcal/mol). This is a substantial difference in energy and one would expect the cis adduct to be formed in high excess at room temperature. Furthermore, in a CPMD simulation in vacuum in which the Ru−N7(G) distance was constrained to 5.5 Å, the guanine moved from a trans to a cis position within 1.7 ps. This demonstrates that the kinetic barrier between the two forms is small. There is no indication of a well-defined minimum in which the guanine N7 and O6 atoms form H-bonds with both hydrogens of the same diamine-NH_2 group. A starting configuration with the O6 (instead of N7) coordinated to the Ru atom is also possible but energetically less favorable. Therefore, the investigation of this alternative cis water exchange reaction mechanism is not included in this study.

1.2. Energetics of the Aqua vs Guanine Ligand Exchange. Having discussed the nature of the reactant adducts, we proceeded with the investigation of the entire exchange reaction in gas phase. Initial constrained linear-transit calculations, in which we progressively shortened the ruthenium−N7(G) distance until the aqua ligand left and the Ru−guanine bond was formed, lead to huge hysteresis effects when the direction of the reaction coordinate was inverted. The arene and the diamine are polydentate and interconnected via the tetrahedral ruthenium coordination center, which leads to a complex PES with many local minima and complex reaction coordinates. Therefore, we applied a combination of free and distance-constrained CPMD simulations at finite temperatures to escape from local minima. In a subsequent step, the obtained structures were quenched to 0K and geometry optimized.

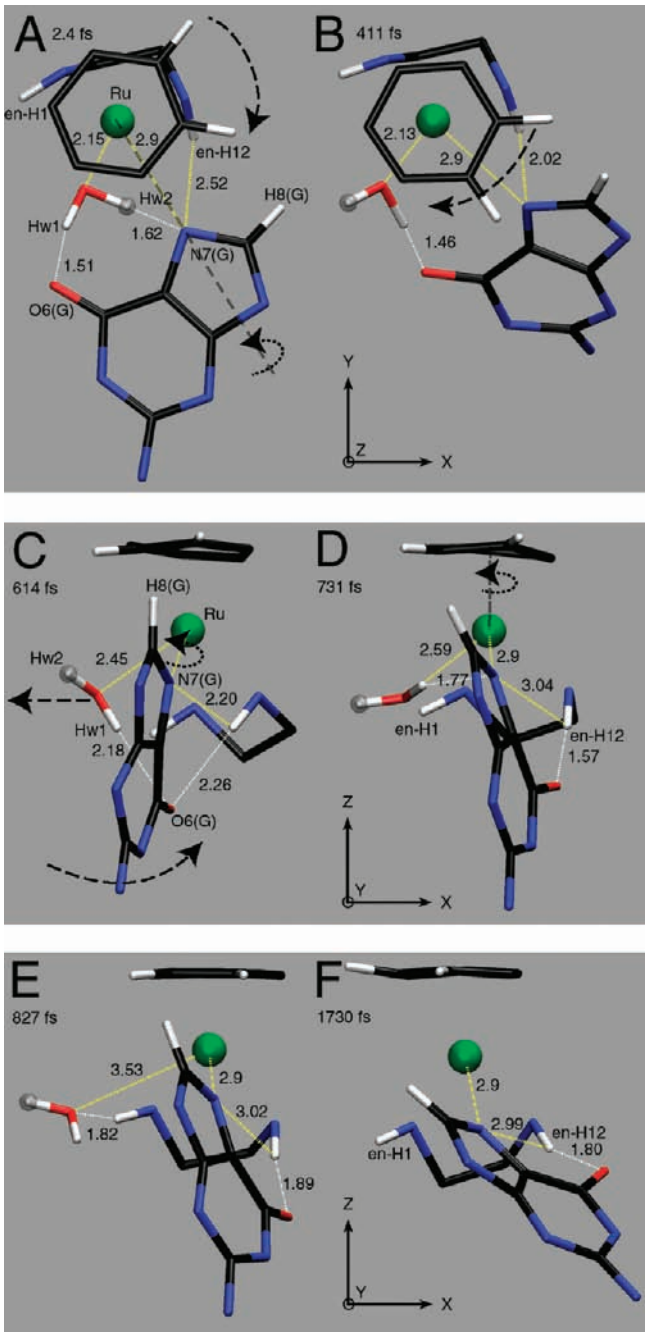

Figure 4. Snapshots of a constrained CPMD trajectory showing the cis aqua vs guanine ligand exchange reaction in the pseudotetrahedral complex **1**. Snapshots A and B show a view along the ruthenium benzene-centroid *z*-axis, C−F show a view perpendicular to this *z*-axis. All ruthenium-ligand bonds and selected hydrogens are omitted for clarity. One hydrogen of the aqua ligand is shown in gray to allow for distinction.

1.2.1. Guanine Cis to Aqua Ligand. Approaching the N7(G) atom from the aqua side of the ruthenium complex, the displacement of the aqua ligand from **1** could be observed by means of a constrained CPMD simulation of 10 ps. Figure 4 shows representative snapshots (A−F) of the ligand exchange reaction, in which the Ru−N7(G) distance was constrained to 2.9 Å.[50] During these simulations, we observed three major rearrangements: (i) a complete detachment of the aqua ligand from the ruthenium complex, (ii) a 180° rotation of the complex around the Ru−N7(G) axis, and (iii) a 180° rotation of the benzene around the ruthenium benzene-centroid axis.

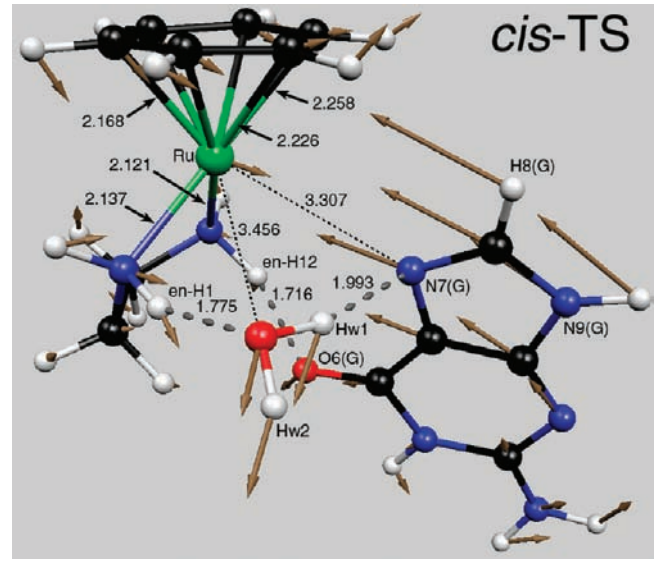

Figure 5. TS of the aqua/guanine ligand exchange reaction starting from the cis reactant adduct. Brown arrows indicate the atomic displacements of the imaginary eigenmode.

Snapshot A shows the reactant adduct with the guanine plane nearly parallel to the benzene plane. The incoming guanine is H-bonding via its O6 and N7 atoms to the aqua hydrogen atoms Hw1 and Hw2, respectively. In B, Hw2 has broken the H-bond to N7(G). The N7(G) does compensate for this broken H-bond by the formation of a new H-bond to the en-H12. The guanine starts turning around the Ru−N7 axis and its O6(G) moves downward, away from the benzene plane. However, it maintains H-bonding to the aqua Hw1. Due to this rotation, the H8(G) atom points up toward the benzene ring and sticks between two aromatic hydrogens. As a consequence of the axial guanine motion, the benzene starts rotating. This concerted motion can be imagined as a molecular gear, where the benzene hydrogen atoms and the H8(G) atom act as teeth. It transfers the torque of the guanine rotation around the Ru−N7 axis into the rotation of the benzene around the ruthenium benzene-centroid axis.

Snapshot C (0.6 ps) is similar to the calculated TS (see Figure 5). The guanine plane is now nearly perpendicular to the benzene plane, which allows for the formation of a maximum number of three H-bonds. In the TS structure, the leaving aqua ligand is still coordinated to the ruthenium center and forms two hydrogen bonds to the N7(G) and the en-H1. The guanine is turned by ∼90° compared to the initial reactant adduct while the N7(G) has partially formed a bond to the ruthenium center (3.31 Å) and the O6(G) forms a H-bond to the en-H12.

After 0.7 ps (D) the aqua ligand starts dissociating. Frame E (0.8 ps) shows the leaving H_2O molecule. It is guided away from the complex via a H-bond to the en-H1. Finally, the H_2O moves away from the complex, completing its evolution from a coordinated ligand to a solvent molecule (F; 1.7 ps). During this simulation, the complex and the benzene ring have turned by 180° compared to the initial reactant adducts (A). We calculated an activation energy of 25.7 kcal/mol in the gas phase (solution, 22.2 kcal/mol; Figures 10 and 11).

Once the aqua ligand has been displaced, further shortening of the Ru−N7(G) distance leads to the formation of the complex $[(\eta^6\text{-benzene})\text{Ru(en)(N7-guanine)}]^{2+}$, which shows the characteristic hydrogen bond between the O6(G) and the diamine H1 (Figure 6). Our gas phase calculations showed that the global energy minimum for the leaving water molecule involves an H-bonded adduct to the guanine H9 atom. This final Ru−N7(G)

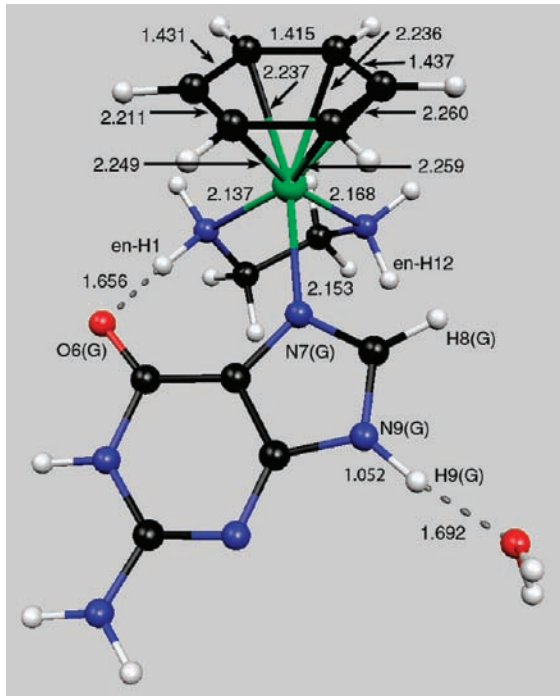

Figure 6. Final reaction product $[(\eta^6\text{-benzene})\text{Ru(en)(N7\{G\})}]^{2+}$ with the explicit water molecule H-bonding to H9(G) showing the characteristic H-bond between O6(G) and en-H1.

product with the explicit solvent water H-bonding to the H9(G) is only slightly more stable (gas phase, 2.8 kcal/mol; solution, 5.5 kcal/mol) than the initial cis reactant adduct (Figure 10 and 11). (The transformation of a coordinated aqua ligand to an explicit solvent water molecule results in a mixed treatment of an explicit quantum water molecule and a continuum water model for the bulk. However, our results show that the error introduced by the continuum description is rather small (1.6 kcal/mol, Figure 11).) Recently, another study reported an alternative TS for the reaction of guanine with **1**.[51] The proposed structure is also a saddle point within our methodology. The H-bond pattern resembles the one of the cis-TS in this work and we calculated for both structures identical energies.

1.2.2. Guanine Trans to Aqua Ligand. Starting from the trans reactant adduct (Figure 2) in which guanine is H-bonding to **1** via the diamine, we identified two different pathways toward the formation of the final Ru−N7(G) product.

Direct Attack at N7(G). The most intuitive way for the formation of the N7(G)−ruthenium product (Figure 6) starting from a trans adduct passes through a TS in which the N7(G) competes directly with the aqua oxygen for a coordination site at the ruthenium center. However, for this reaction to occur, the complex has to change one leg of its tripod. Consequently, the arene and the chelating diamine have to "flip" from a $O_{aqua}-N_{en}-N_{en}$ to a $N_{en}-N_{en}-N7(G)$ piano stool geometry.

This flip involves a TS in which the plane spanned by the ruthenium and the two diamine nitrogen atoms is perpendicular to the benzene plane. The arrows in Figure 7 indicate one of the two opposite directions of the displacement associated to the negative vibrational frequency of the TS. The concerted flip of the arene and the diamine moieties opens the way for the incoming guanine ligand. This TS allows for the formation of a H-bond between an en-NH_2 hydrogen and the N7(G) (2.03 Å, 155.1°). The benzene ring is not completely planar but adopts a slightly concave geometry bent toward the ruthenium center. The H-bond between the O6(G) and an en-NH_2 hydrogen atom, which is characteristic for the final Ru−N7(G) product,[31,32] is

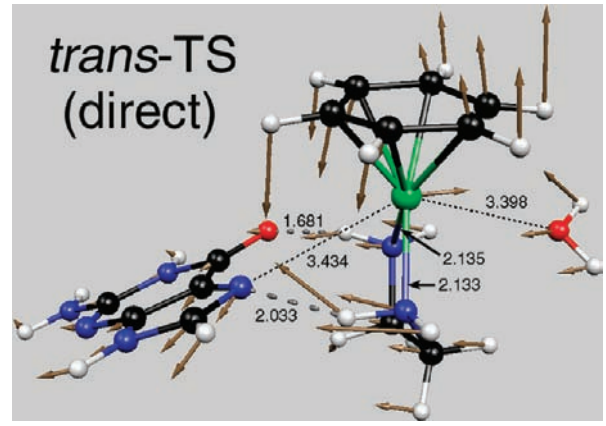

Figure 7. Transition state of the trans-direct ligand exchange reaction of **1** with guanine. Arrows indicate one of the two directions of the displacement associated to the negative vibrational frequency.

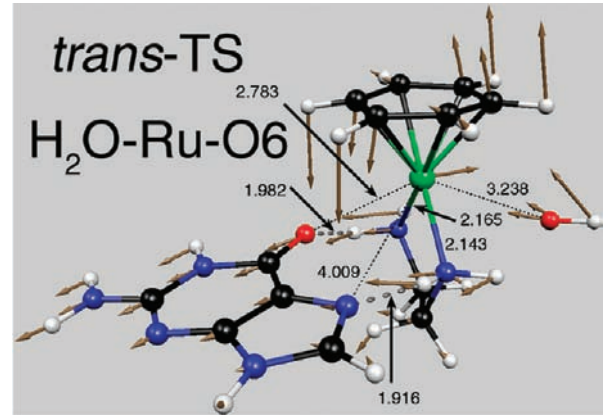

Figure 8. Transition state of a ligand exchange reaction in which the O6(G) atom replaces the aqua ligand in **1**.

already fully established (1.681 Å, 163.8°). This trans-direct TS is higher in energy than the cis TS discussed above both in the gas phase (6.5 kcal/mol) and in solution (7.4 kcal/mol) (Figure 10 and 11). Further shortening of the distance between the N7(G) and the ruthenium center yields again the final product $[(\eta^6\text{-benzene})\text{Ru(en)(N7\{G\})}]^{2+}$ (Figure 6).

Two Step Mechanism via an O6(G) Intermediate. The trans-direct pathway described above is not the only pathway that leads to the formation of the Ru−N7(G) complex starting from the trans reactant adduct (Figure 2). We identified a second reaction pathway that proceeds instead through an intermediate where the O6(G) binds to the ruthenium center (Figure 9). Starting from the trans reactant adduct, it is the O6(G) that initially replaces the aqua ligand. The TS involved is similar in its structure to the trans-direct TS discussed above, but this time it is the N7(G) that forms a strong H-bond (1.916 Å, 157.0°) with the en-NH_2 group (Figure 8).[33] The Ru−OH_2 distance (3.238 Å) is 0.16 Å shorter than in the trans-direct TS and 0.22 Å shorter than in the cis TS. Interestingly, the (G)O6−Ru distance (2.783 Å) is much shorter than the (G)N7−Ru distance (3.434 Å) in the trans-direct TS, suggesting that the reaction mechanism is more associative for O6(G) than for N7(G). Like in the trans-direct TS, the arene is bent toward the ruthenium center and the plane spanned by the N(en)−Ru-N(en) atoms is perpendicular to the arene plane. A normal-mode analysis shows that the incoming and leaving oxygen atoms of the two ligands are moving nearly along the same O−Ru−O axis (Figures 8 and S4 (Supporting Information)). Like in the case of the trans-

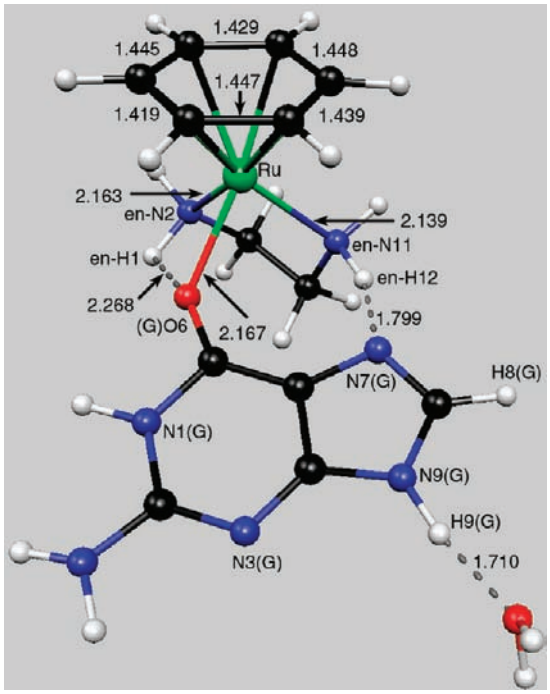

Figure 9. Intermediate $[(\eta^6\text{-benzene})Ru(en)(O6\{G\})]^{2+}$ with the solvent water H-bonding to H9(G).

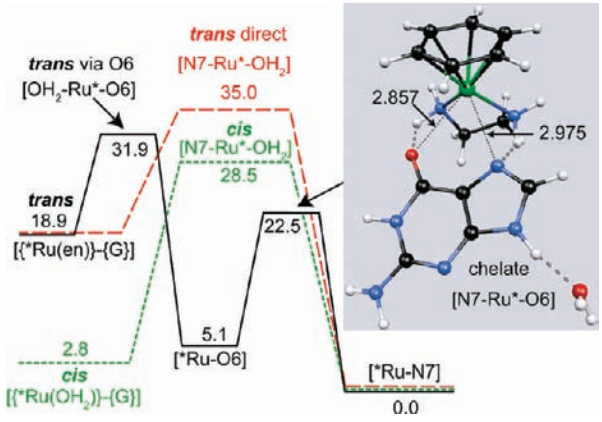

Figure 10. Relative gas phase energies of the three investigated reaction pathways that lead to the formation of $[(\eta^6\text{-benzene})Ru(en)(N7\{G\})]^{2+}$.

direct pathway, the "flipping" movement of the arene and diamine ligand is observed.

Decreasing the (G)O6−Ru distance further results in a guanine−ruthenium complex, in which the guanine is coordinated via its O6 atom to the ruthenium center and the N7(G) forms a strong H-bond (1.799 Å, 161.0°) to the diamine en-H12. This compound exists in two stable diamine conformations (for details see ref 33). The energy difference between these two conformers amounts to 1.4 kcal/mol and the most stable conformer is the one depicted in Figure 9. In this conformer, the O6(G) not only forms a coordinative Ru−O6(G) bond but also is involved in the formation of a H-bond to the en-H1 (2.268 Å, 104.4°).

In a previous study we showed that this Ru−O6(G) intermediate can undergo an intramolecular ligand exchange reaction via a TS in which both guanine O6 and N7 atoms are chelated to the ruthenium center (Figure 10).[47] In addition to this chelatization, the O6(G) and N7(G) atoms are simultaneously involved in the formation of two H-bonds with the diamine ligand (N7, 2.205 Å, 130.9°; O6, 1.980 Å, 124.4°). This

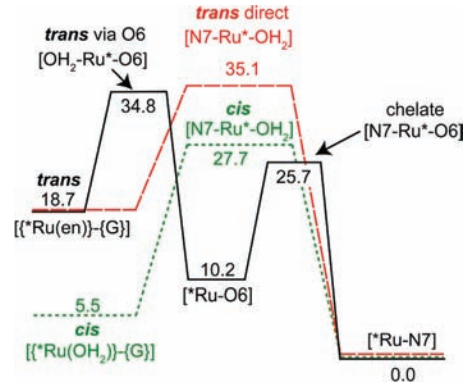

Figure 11. Relative solution energies (COSMO) of the three investigated reaction pathways that lead to the formation of $[(\eta^6\text{-benzene})Ru(en)(N7\{G\})]^{2+}$.

chelating TS [N7−Ru−O6] is ∼9 kcal/mol lower in energy (both in vacuo and in solution) than the trans H_2O−Ru−O6(G) TS in this two-step mechanism.

1.3. Reaction Profiles. The resulting energy profiles for the three reaction pathways in gas phase and in solution are shown in Figures 10 and 11, respectively.

For both gas phase and solution energy profiles, the trans-direct (gas, 32.2 kcal/mol; solution, 29.6 kcal/mol) and trans-via-O6 pathway (gas, 29.1 kcal/mol; solution, 29.3 kcal/mol) imply overall higher activation energy barriers than the cis pathway (gas, 25.7 kcal/mol; solution, 22.2 kcal/mol). In addition, the cis reactant adduct is far more stable than the trans adduct. The overall energy profiles computed in the gas phase and solution are very similar (the maximum difference between gas phase and solution results is 5.1 kcal/mol). Free energy calculations for the transition states confirmed that the relative energy differences are maintained also at room temperature.

2. Docking Studies to DNA. ***2.1. Docking Study of Ru−Aqua with dsDNA.*** In highly flexible single-stranded (ss) DNA, the N7 atom of guanine constitutes the main target for hydrolyzed $[(\eta^6\text{-arene})Ru(en)(Cl)]^+$ complexes.[29,52] However, the predominant cellular DNA form is double stranded (ds) DNA. The latter is more rigid due to Watson−Crick base pairing of the complementary strands. As shown in a molecular dynamics study elsewhere, docking revealed that **1** can hardly approach its guanine-N7 target via the minor groove, as this implies substantial breaking of Watson−Crick hydrogen bonds.[47] The wider major groove, however, allows for a direct access to the N7(G) atom (Chart S1, Supporting Information).

In a qualitative rigid docking study we investigated the potential pathways of the Ru−aqua complex toward the N7(G) atom in a B-DNA model starting from the previously determined H-bonded DNA adduct precursor. To this end, we fitted the H-bonded cis and trans adduct structures of guanine with **1** (Figures 1 and 2) to one of the central guanine bases in the dsDNA 12-mer d(CCTCTG*GTCTCC)/d(GGAGACCAGAGG). Taking into account the possible cis and trans adduct formation as well as the 5′ and 3′ directionality of the DNA, four cases have to be considered.

Our qualitative results show that these four theoretical adducts fit indeed into dsDNA (Figures 12 and S5 (Supporting Information)). No steric clashes occur, whether the ruthenium bound arene is oriented toward the 5′- or the 3′-direction of the DNA strand. In the case of a trans attack, both amino groups of the diamine ligand can form H-bonds with the guanine N7 or C6═O atoms. Consequently, the aqua ligand points out of the major groove toward the bulk water.

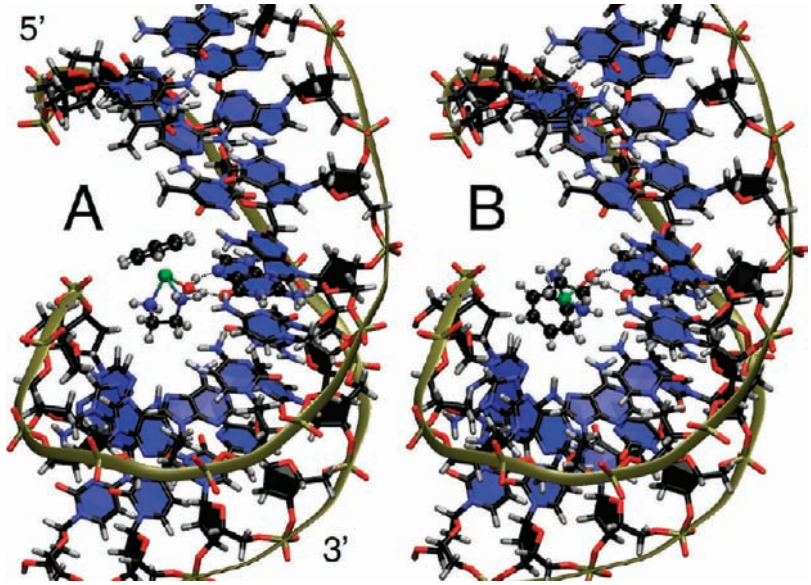

Figure 12. Cis adducts of guanine (balls and sticks) and **1** fitted to guanine in dsDNA (sticks and ribbon). The ruthenium bound arene is oriented in 5′- or in 3′- direction (A and B, respectively) relative to the DNA strand.

2.2. Docking of the Calculated TSs into dsDNA. The identified gas phase TSs give a first indication of the energies involved in the reaction of $[(\eta^6\text{-benzene})Ru(en)(OH_2)]^{2+}$ with guanine. However, the biologically relevant target is a guanine in solvated dsDNA. This realistic environment provides additional possibilities for strain energy, more potential H-bonds, as well as hydrophobic and electrostatic interactions. To get a qualitative understanding of the relevance of the gas phase TS structures, we superimposed the corresponding ruthenium-guanine TS complexes with a guanine base in dsDNA. As pointed out earlier, in these structures the $[(\eta^6\text{-benzene})Ru(en)(OH_2)]^{2+}$ moiety is coordinated not only to the guanine via direct coordination bonds to ruthenium but also via at least one additional H-bond to N7(G) or O6(G) of the aqua or diamine ligands, which substantially limits the docking possibilities. As shown elsewhere, these H-bonds are maintained also in explicit solvent at 310 K.[47]

None of the fitted four gas phase TS structures collide directly with parts of the dsDNA. However, some TSs show very close contacts when docked rigidly into dsDNA. The unfavorable interactions cannot be easily removed by geometrical relaxations. In particular, the TS structure of the trans-via-O6 reaction pathway shows numerous repulsive steric interactions. This is because in dsDNA, the guanine O6 atom is involved in Watson−Crick hydrogen bonding with a cytosine C4−NH_2 of the complementary strand (Chart S1, Supporting Information). Superimposing the gas phase (G)O6−Ru−OH_2 TS resulted in distances between DNA fragments and the ruthenium complex as close as 1.3 and 0.7 Å in 5′ and 3′ orientation, respectively (Figure S6, E and F, Supporting Information). The O6−Ru−N7 TS does not show significant steric limitations if the benzene ligand of the ruthenium complex is oriented along 5′-direction of the DNA strand to which it is bound (Figure S6, G, Supporting Information). In contrast, a 3′-orientation results in intermolecular distances as close as 1.5 Å (Figure S6, H, Supporting Information).

The cis TS in which the leaving aqua ligand is oriented in 5′-direction (Figure S6, B, Supporting Information) is also unfavorable since the exit pathway of the leaving aqua ligand is blocked by the surrounding dsDNA. However, if the aqua ligand is oriented in 3′-direction (Figure 13, A), the water molecule can easily leave the reaction site, diffusing into water of the major groove. In this case, the closest contact involves one of the benzene hydrogens, which is as close as 2.2 Å from the C5-methyl carbon of an adjacent thymine.

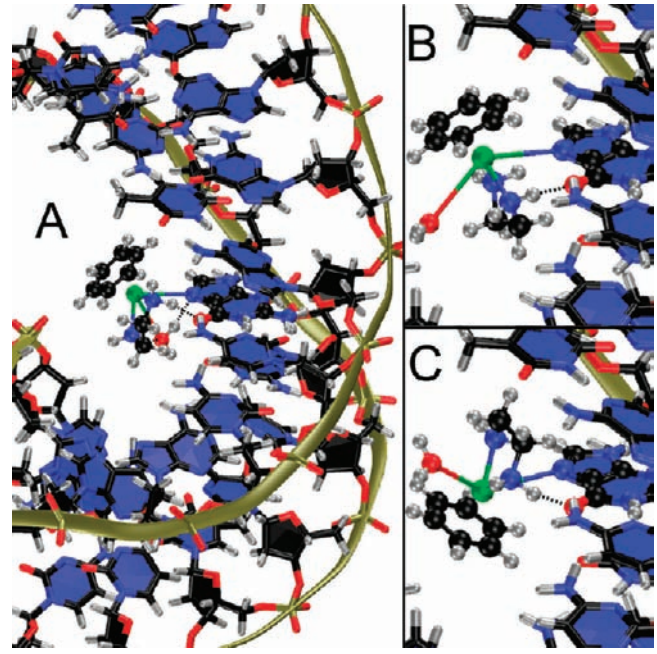

Figure 13. Superposition of gas phase ruthenium−guanine TSs with guanine in dsDNA. The cis TS with the leaving aqua ligand in 3′-direction (A) and the trans-direct TS with the benzene in 5′- and 3′-direction (B and C, respectively). The black dashed H-bonds show the interactions of the ruthenium complex with the bound guanine in the TS as in Figures 5, 7 and 8, respectively.

For both orientations of the trans-direct TS, the water molecule can leave the reaction site even easier, diffusing into the major groove water without any steric hindrance. The only steric interactions observed in this case involve the methylene hydrogen atoms of the diamine ligand in the ruthenium complex. More precisely, in the case of the benzene ligand oriented along the 5′-direction, these form a close contact (1.9 Å) with the adenine C6−NH_2 group in the complementary strand and with the adjacent O6(G) atom (1.8 Å) in the same strand (Figure 13,

CHART 1: Schematic Drawing of Initial (A, C) and Final (B, D) CPMD Structures Showing an Irreversible Proton Transfer from the Aqua Ligand to the Adenine N1 and N7 Atoms, Respectively

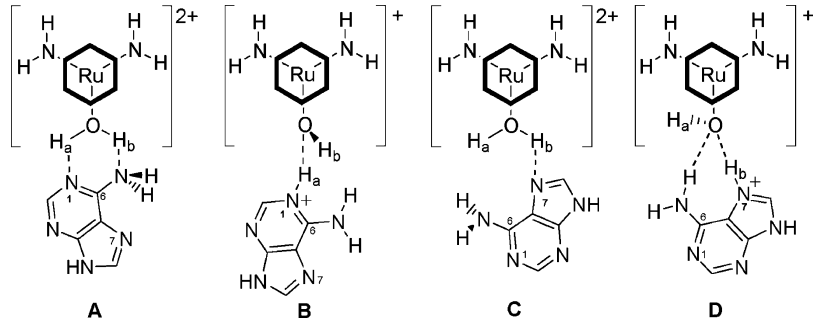

CHART 2: Schematic Drawing of H-Bonded Adducts Observed during a CPMD Trajectory Started from Cytosine in Trans and Cis Position to the Aqua Ligand (Initial, A and C; Final, B and D), Respectively

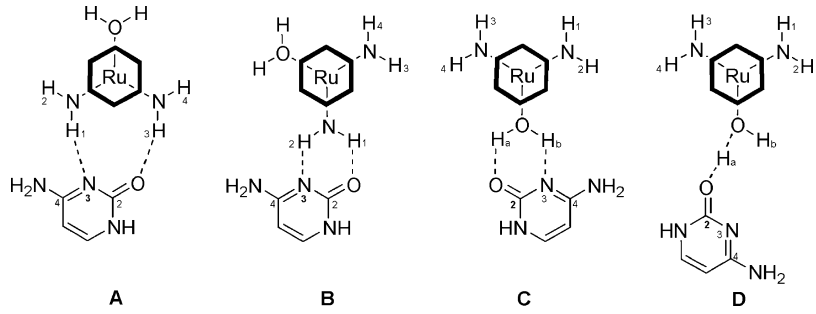

B). When the benzene ligand is oriented toward the 3′-direction, the same diamine hydrogen atoms approach the C5 atom of an adjacent thymine up to distances of 2.0 Å (Figure 13, C).

In summary, this qualitative study shows that only the trans-direct TS and the cis TS with the aqua ligand oriented in 3′-direction are promising candidates for a reaction pathway from the Ru-aqua compound to the Ru-DNA adduct.

3. Reactions of Ru−Aqua with Adenine and Cytosine. ***3.1. Adenine.*** In analogy to the reaction with guanine, we performed CPMD simulations and geometry optimizations for the trans and cis reactant adducts. Surprisingly, we found that the interaction of **1** with adenine is very different from the one with guanine. The experimentally determined pK_a (7.71) of the related compound $[(\eta^6\text{-biphenyl})Ru(en)(OH_2)]^{2+}$ suggests that only small amounts of the less reactive hydroxo species would be present at biological pH (∼7.3).[28] In contrast, we observed a significantly increased acidity of **1** in the gas phase.

3.1.1. Trans-Adduct. Geometry optimizations of structures in which adenine faces the diamine side of the ruthenium complex with the lone pairs of the N7(A) atom and of the C6−NH_2(A) group yield a weakly H-bonded reactant adduct (Chart S2, A, Supporting Information). However, in contrast to the case of guanine, we did not observe any stable H-bonded trans adduct.

During the CPMD simulation, the adenine migrated spontaneously toward the aqua (cis) side of the ruthenium complex, where both its N7 atom and the C6−NH_2 group can form a H-bond to both hydrogen atoms of the aqua ligand (Chart S2, C, Supporting Information). Remarkably, in this temporary configuration, we observed several times the reversible formation of an adenine C6−NH_3^+ ammonium cation by deprotonation of the aqua ligand and protonation of C6−NH_2(A) (Figure S7, Supporting Information). A similar proton transfer was also observed in a computational study on the reaction of a cisplatin hydrolysis product with guanine and adenine.[53]

3.1.2. Cis-Adduct. We started our investigations from two different initial structures which allow either the N1 or the N7 positions of adenine to interact with the aqua ligand of **1** (Chart 1, A and C, respectively).

N1-Protonation. Geometry optimizations at 0 K revealed a sp^3 hybridization of the C6−NH_2 group which allows for H-bonding with the aqua ligand of **1** (Chart 1, A). However, in our CPMD trajectory we observed an immediate, spontaneous and irreversible deprotonation of the aqua ligand and a protonation of N1(A) when adenine approaches **1** with its N1 atom and the C6−NH_2 group from the cis side of the aqua ligand (Chart 1, B). The proton on the N1(A) atom forms a H-bond to the oxygen of the hydroxo ligand. However, this bond length is constantly increasing during the dynamics which is a clear indication of its thermal instability (Figure S8, Supporting Information).

N7-Protonation. Starting from configuration C in Chart 1, we observed in simulations at 80 K an immediate, spontaneous and irreversible deprotonation of the aqua ligand. It is the N7(A) atom, which is protonated in this configuration (D in Chart 1, Figure S9, Supporting Information). At low temperature, the resulting H-bonding pattern keeps both molecules together. However, heating the system up to 310 K resulted in a rupture of the hydrogen bonds within only 0.4 ps, and the protonated adenine separated from the ruthenium complex (Figure S9, Supporting Information).

These results suggest that adenine gets protonated in its N1 or N7 positions when approaching the aqua species of the ruthenium complex in vacuo. The acidic ruthenium aqua complex is deprotonated and forms a hydroxo species. The resulting N1-protonated adenine adduct is ∼7.8 kcal/mol more stable than the N7 protonated adduct. However, solvation effects might stabilize the unprotonated adenine in the adduct with **1**. Calculations, in which we applied the COSMO methodology also for geometry optimizations, suggest that the N1-protonated form and the unreacted adenine adduct with **1** are equally stable. In the case of the N7 atom, the adduct containing the unprotonated adenine ligand is even slightly more stable (2 kcal/

mol) than the N7 protonated adduct. These initial calculations show the importance of solvation effects for the basicity of adenine.

3.2. Cytosine. We also investigated H-bonded adducts that are formed during a cis and trans approach of the aqua ligand in **1** to cytosine.

3.2.1. Trans-Adduct. In contrast to guanine and like in the case of adenine, we never observed in our CPMD simulation (80 K) a stable adduct with cytosine trans to the aqua ligand. Instead, the cytosine moved toward the aqua side of **1** (Chart 2), as observed in the case of adenine.

3.2.2. Cis-Adduct. During our CPMD simulation (80 K) started with a cytosine placed in cis position with respect to the aqua ligand (Chart 2, C), we observed a breakdown of the H-bond between the cytosine N3 and the aqua H_b within the first 0.4 ps. The interaction between the cytosine C2═O and the aqua H_a atom, however, is much stronger. In fact, analysis of the $O_{aq}-H_a$ bond revealed that the H_a oscillates between the cytosine C2═O and the aqua oxygen (Figure S10, Supporting Information). However, in contrast to the deprotonation of the aqua ligand that we observed in the case of adenine, the proton remains mainly at the aqua site in the case of cytosine.

Conclusions

We have examined computationally the binding of the anticancer compound $[(\eta^6\text{-benzene})\text{Ru(en)}(\text{OH}_2)]^{2+}$ (**1**) to the nucleobases guanine, adenine, and cytosine. Due to the very complex PES caused by numerous interconnected H-bonds, a computational approach was indicated that permits extended sampling with the help of ab initio molecular dynamics.

Our simulations show that a reactant adduct of **1** and guanine can be formed in which the N7(G) and O6(G) atom form H-bonds either to both aqua hydrogen atoms (cis-adduct) or to the exohydrogen atoms of both diamine-NH_2 groups (trans-adduct). In agreement with ref 51, we found that the cis-adduct is thermodynamically more stable and that the cis reaction pathway is kinetically preferred in both the gas phase and solution. The TSs in which the incoming N7(G) replaces the leaving aqua ligand are neither associative nor dissociative but reflect more an interchange character.

Docking studies show that **1** can reach a N7(G) atom in dsDNA via the major groove and that both TSs, the one for the cis and the trans reaction pathways, can be docked into the DNA environment without steric hindrance.

In full agreement with experimental observations, our results suggest that guanine is more reactive to **1** than adenine and cytosine. In the gas phase, the N7/N1(A) atoms or O2(C) atom get deactivated by protonation while the N7(G) atom does not. This in vacuo protonation of adenine and cytosine results in the formation of the less reactive hydroxo species of **1**.[32] As a consequence, neither the protonated adenine nor the deactivated cytosine are likely to react with the ruthenium center. However, solvation can reduce the basicity of the nucleobase significantly, as was shown in the case of adenine. The drug induced nucleobase selectivity observed in the gas phase is therefore unlikely to be relevant in polar solvents.

Finally, we showed that the arene in **1** can rotate freely and it can even act as a molecular gear during a cis reaction with guanine. It was also shown that the diamine in **1** can adapt its dihedral angle to the molecular environment. Both properties could be of importance for the reaction of **1** with nuclear DNA in a cellular environment.

Acknowledgment. Support from the Swiss National Science Foundation (Grant No 200021-100242/1) is gratefully acknowledged.

Supporting Information Available: Figures S1-S10 with additional information on the dynamics of compound 1/DNA-base complex formation and corresponding structural properties (figures are referred in the main text). Charts S1-S2 indicate the main metal binding sites found in DNA and the hydrogen bond networks observed between compound 1 and guanine during a CPMD trajectory. This material is available free of charge via the Internet at http://pubs.acs.org.

References and Notes

(1) Rosenberg, B.; Camp, L. v.; Krigas, T. *Nature* **1965**, *205*, 698–699.
(2) Reedijk, J. *Chem. Commun.* **1996**, 801–806.
(3) Wong, E.; Giandomenico, C. M. *Chem. Rev.* **1999**, *99*, 2451–2466.
(4) Fuertes, M. A.; Alonso, C.; Pérez, J. M. *Chem. Rev.* **2003**, *103*, 645–662.
(5) Clarke, M. J.; Zhu, F.; Frasca, D. R. *Chem. Rev.* **1999**, *99*, 2511–2533.
(6) Galanski, M.; Arion, V. B.; Jakupec, M. A.; Keppler, B. K. *Curr. Pharm. Des.* **2003**, *9*, 2078–2089.
(7) Haiduc, I.; Silvestru, C. *Coord. Chem. Rev.* **1990**, *99*, 253–96.
(8) Guo, Z.; Sadler, P. J. *Angew. Chem., Int. Ed. Engl.* **1999**, *38*, 1512–1531.
(9) Wang, D.; Lippard, S. J. *Nature Rev. Drug Discovery* **2005**, *4*, 307–320.
(10) Allardyce, C. S.; Dyson, P. J. *Platinum Metals. Rev.* **2001**, *45*, 62–69.
(11) Sava, G.; Capozzi, I.; Clerici, K.; Gagliardi, G.; Alessio, E.; Mestroni, G. *Clin. Exp. Met.* **1998**, *16*, 371–379.
(12) Rademaker-Lakhai Jeany, M.; van den Bongard, D.; Pluim, D.; Beijnen Jos, H.; Schellens Jan, H. M *Clin. Cancer Res.* **2004**, *10*, 3717–27.
(13) Kapitza, S.; Pongratz, M.; Jakupec, M. A.; Heffeter, P.; Berger, W.; Lackinger, L.; Keppler, B. K.; Marian, B. *J. Cancer Res. Clin. Oncol.* **2005**, *131*, 101–110.
(14) Hartinger, C. G.; Zorbas-Seifried, S.; Jakupec, M. A.; Kynast, B.; Zorbas, H.; Keppler, B. K. *J. Inorg. Biochem.* **2006**, *100*, 891.
(15) Dyson, P. J.; Sava, G. *Dalton Trans.* **2006**, 1929–1933.
(16) Yan Yaw, K.; Melchart, M.; Habtemariam, A.; Sadler, P. J. *Chem. Commun.* **2005**, *476*, 4–76.
(17) Allardyce, C. S.; Dyson, P. J.; Ellis, D. J.; Heath, S. L. *Chem. Commun.* **2001**, 1396–1397.
(18) Wang, F.; Habtemariam, A.; van der Geer, E. P. L.; Fernandez, R.; Melchart, M.; Deeth, R. J.; Aird, R.; Guichard, S.; Fabbiani, F. P. A.; Lozano-Casal, P.; Oswald, I. D. H.; Jodrell, D. I.; Parsons, S.; Sadler, P. J. *Proc. Natl. Acad. Sci. U.S.A.* **2005**, *102*, 18269–18274.
(19) Scolaro, C.; Bergamo, A.; Brescacin, L.; Delfino, R.; Cocchietto, M.; Laurenczy, G.; Geldbach, T. J.; Sava, G.; Dyson, P. J. *J. Med. Chem.* **2005**, *48*, 4161–4171.
(20) Gopal, Y. N. V.; Jayaraju, D.; Kondapi, A. K. *Biochemistry* **1999**, *38*, 4382–4388.
(21) Gaiddon, C.; Jeannequin, P.; Bischoff, P.; Pfeffer, M.; Sirlin, C.; Loeffler, J. P. *J. Pharmacol. Exp. Ther.* **2005**, *315*, 1403–1411.
(22) Huxham, L. A.; Cheu, E. L. S.; Patrick, B. O.; James, B. R. *Inorg. Chim. Acta* **2003**, *352*, 238–246.
(23) Akbayeva, D. N.; Gonsalvi, L.; Oberhauser, W.; Peruzzini, M.; Vizza, F.; Brueggeller, P.; Romerosa, A.; Sava, G.; Bergamo, A. *Chem. Commun.* **2003**, 264–265.
(24) Romerosa, A.; Campos-Malpartida, T.; Lidrissi, C.; Saoud, M.; Serrano-Ruiz, M.; Peruzzini, M.; Garrido-Cardenas, J. A.; Garcia-Maroto, F. *Inorg. Chem.* **2006**, *45*, 1289–1298.
(25) Serli, B.; Zangrando, E.; Gianferrara, T.; Scolaro, C.; Dyson, P. J.; Bergamo, A.; Alessio, E. *Eur. J. Inorg. Chem.* **2005**, *342*, 3–3434.
(26) Aird, R. E.; Cummings, J.; Ritchie, A. A.; Muir, M.; Morris, R. E.; Chen, H.; Sadler, P. J.; Jodrell, D. I *Br. J. Cancer* **2002**, *86*, 1652–1657.
(27) Habtemariam, A.; Sadler, P. J., 2005-GB3242, 2006018649, 20050819, 2006.
(28) Wang, F.; Chen, H.; Parsons, S.; Oswald, I. D. H.; Davidson, J. E.; Sadler, P. J. *Chem.—Eur. J.* **2003**, *9*, 5810–5820.
(29) Wang, F.; Bella, J.; Parkinson, J. A.; Sadler, P. J. *J. Biol. Inorg. Chem.* **2005**, *10*, 147–155.
(30) Wang, F.; Xu, J.; Habtemariam, A.; Bella, J.; Sadler Peter, J. *J. Am. Chem. Soc.* **2005**, *127*, 17734–43.
(31) Chen, H.; Parkinson, J. A.; Parsons, S.; Coxall, R. A.; Gould, R. O.; Sadler, P. J. *J. Am. Chem. Soc.* **2002**, *124*, 3064–3082.
(32) Chen, H.; Parkinson, J. A.; Morris, R. E.; Sadler, P. J. *J. Am. Chem. Soc.* **2003**, *125*, 173–186.
(33) Gossens, C.; Tavernelli, I.; Rothlisberger, U. *J. Chem. Theory Comp.* **2007**, *3*, 1212–1222.

(34) Dorcier, A.; Dyson, P. J.; Gossens, C.; Rothlisberger, U.; Scopelliti, R.; Tavernelli, I. *Organometallics* **2005**, *24*, 2114–2123.

(35) Scolaro, C.; Geldbach, T. J.; Rochat, S.; Dorcier, A.; Gossens, C.; Bergamo, A.; Cocchietto, M.; Tavernelli, I.; Sava, G.; Rothlisberger, U.; Dyson, P. J. *Organometallics* **2006**, *25*, 756–765.

(36) *ADF 2004.01; SCM, Theoretical Chemistry*; Vrije Universiteit: Amsterdam, The Netherlands, 2004; http://www.scm.com.

(37) Becke, A. D. *Phys. Rev. A* **1988**, *38*, 3098–100.

(38) Perdew, J. P. *Phys. Rev. B* **1986**, *33*, 8822–8824.

(39) Lenthe, E. v.; Ehlers, A. E.; Baerends, E. J. *J. Chem. Phys.* **1999**, 110.

(40) *CPMD*, Copyright IBM Corp 1990−2006; Copyright MPI für Festkörperforschung Stuttgart 1997−2001.

(41) Troullier, N.; Martins, J. L. *Phys. Rev. B* **1991**, *43*, 1993–2006.

(42) Except noted otherwise all pseudopotentials were the ones provided in the PP-library of CPMD (www.cpmd.org).

(43) Maurer, P.; Magistrato, A.; Rothlisberger, U. *J. Phys. Chem. A* **2004**, *108*, 11494.

(44) Kleinman, L.; Bylander, D. M. *Phys. Rev. Lett.* **1982**, *48*, 1425–8.

(45) Gossens, C.; Tavernelli, I.; Rothlisberger, U. *Chimia* **2005**, *59*, 81–84.

(46) Colombo, M. C.; Gossens, C.; Tavernelli, I.; Rothlisberger, U. From Enzymatic Catalysis to Anticancer Drugs: QM/MM Car-Parrinello Simulations of Biological Systems. In *Modelling Molecular Structure and Reactivity in Biological Systems*; Naidoo, K. J., Brady, J., Field, M., Gao, J., Hann, M., Eds.; Royal Society of Chemistry; Cambridge, U.K., 2006; Special Vol. WATOC 2005, pp 85.100.

(47) Gossens, C.; Tavernelli, I.; Rothlisberger, U. *J. Am. Chem. Soc.* **2008**, *130*, 10921–10928.

(48) Flükiger, P.; Lüthi, H. P.; Portmann, S.; Weber, J. *MOLEKEL* 4.0;Swiss Center for Scientific Computing: Manno, Switzerland, 2000.

(49) Humphrey, W.; Dalke, A.; Schulten, K. *J. Mol. Graph.* **1996**, *14*, 33–38.

(50) This distance is 0.4 Å shorter than in the TS (Figure 5) but allowed the reaction to occur spontaneously within the time scale of our simulation. Longer constrained distances did not yield a reaction on a picosecond timescale (e.g., 2.95 Å at 310−500 K during 2.7 ps), while shorter distances caused the aqua ligand to detach rapidly.

(51) Deubel, D. V.; Lau, J. K.-C. *Chem. Commun.* **2006**, 2451–2453.

(52) Morris, R. E.; Aird, R. E.; Murdoch, P. d. S.; H; Chen, J. C.; Hughes, N. D.; Parsons, S.; Perkin, A.; Boyd, G.; Jodrell, D. I.; Sadler, P. J. *J. Med. Chem.* **2001**, *44*, 3616–3621.

(53) Raber, J.; Zhu, C. B.; Eriksson, L. A. *J. Phys. Chem. B* **2005**, *109*, 11006.

JP903237W